*Supporting Information for:*

# Faradaic Counter for Liposomes Loaded with Potassium, Sodium Ions, or Protonated Dopamine

Linhan Huang,[1] Jingcheng Zhang,[1] Zhipeng Xiang,[2] Di Wu,[1] Xinjian Huang,[3] Xizhe Huang,[1] Zhenxing Liang,[2] Zhen-Yu Tang,[4] and Haiqiang Deng[1,*]

[1]School of Chemical Engineering and Technology, Sun Yat-sen University, Zhuhai 519082, China
[2]Key Laboratory on Fuel Cell Technology of Guangdong Province, School of Chemistry and Chemical Engineering, South China University of Technology, Guangzhou 510641, China
[3]Institute of Intelligent Perception, Midea Corporate Research Center, Foshan 528311, China
[4]School of Pharmaceutical Science (Shenzhen), Sun Yat-sen University, Guangzhou 510275, China

*Corresponding author, email: denghq9@mail.sysu.edu.cn (H. Deng).

## *Table of Contents:*

**Table S1.** Parameters for one-stage pulling ~ 600 nm inner-diameter (i.d.) micropipettes from borosilicate glass capillaries (outer/inner diameter: 1.0 mm/0.58 mm, 10 cm length) using a PC-100 puller (Narishige Instrument, Japan).

| No. 1 Heater Level | No. of pulling |
|---|---|
| 51 | 1 |

**Table S2.** Parameters for pulling ~ 6 μm i.d. short-shank micropipettes from borosilicate glass capillaries (outer/inner diameter: 1.0 mm/0.58 mm, 10 cm length) using a P-2000 laser puller (Sutter Instrument, Novato, CA).

| Heat | Filament | Velocity | Pull | Delay |
|---|---|---|---|---|
| 265 | 4 | 26 | 0 | 250 |
| 265 | 4 | 26 | 0 | 250 |
| 265 | 4 | 26 | 0 | 250 |
| 265 | 4 | 22 | 0 | 250 |

**Cell S-I：** Ag| AgCl|20 mM DB18C6 + 5 mM BATB + DCE (inside the micropipette)||10 mM LiCl + 181 pM liposomes (hydrated by 10 mM KCl)|AgCl|Ag

**Cell S-II：** Ag| AgCl|0.5 mM DB18C6 + 5 mM BATB + DCE||10 mM LiCl + 62 pM OVA-liposomes (hydrated by 10 mM DAHCl)|AgCl|Ag

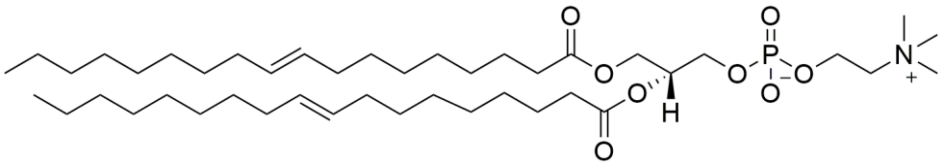

**Figure S1.** Chemical structure of 1,2-dioleoyl-sn-glycero-3-phosphocholine (DOPC).

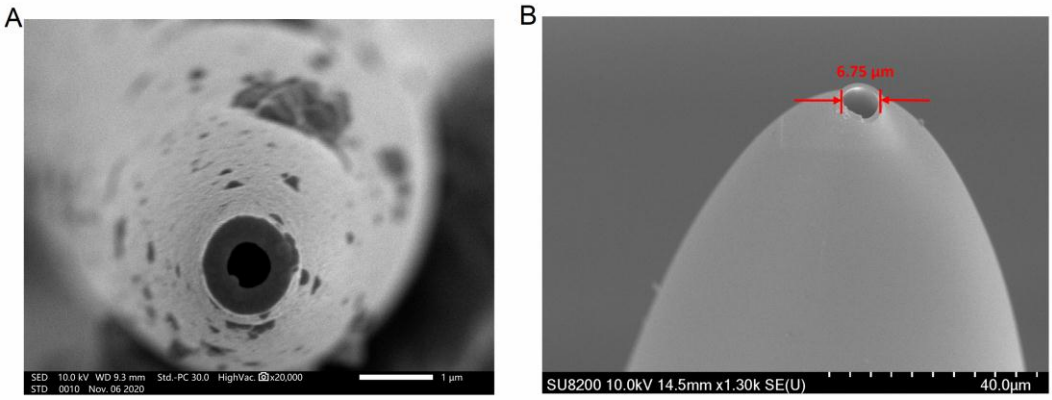


**Figure S2**. SEM images of (A) a 600 nm i.d. sub-micropipette pulled by a PC-100 puller with parameters detailed in Table S1 and (B) a typical micropipette used for electrochemical collisional experiments, i.d. = 6.75 µm, pulled by a P-2000 laser puller with parameters detailed in Table S2.

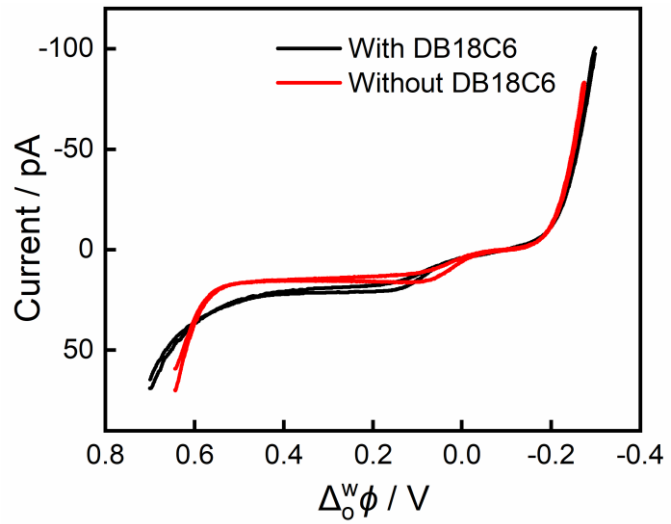


**Figure S3.** CVs (scan rate: 20 mV $s^{-1}$) recorded at a micro-ITIES (i.d. = 600 nm), in which the aqueous phase was 10 mM LiCl + 2 mM TEACl and without ion-contained liposomes, and the organic phase was 5 mM BATB with (black trace) or without (red trace) 0.5 mM DB18C6 in 1,2-dichloroethane (DCE). Note that the potential was converted to the Galvani potential scale, based on CV measurement of the reversible half-wave potential of the $TEA^+$ ion transfer (0.019 V at the $H_2O$/DCE interface, cf. *Electrochimica Acta* 1990, 35, 1173-1175).

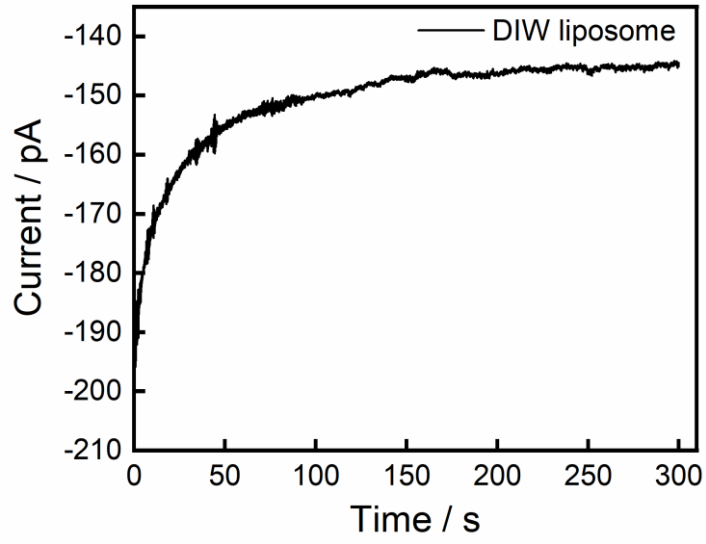


**Figure S4**. Representative *i*−*t* curve for micro-ITIES (i.d. = 8.2 μm) collisional experiments recorded at +0.6 V vs. Ag/AgCl with water-loaded liposomes. The aqueous supporting electrolyte inside the micropipette was 10 mM LiCl, the organic phase was composed of 5 mM BATB + 0.5 mM DB18C6 in DCE.

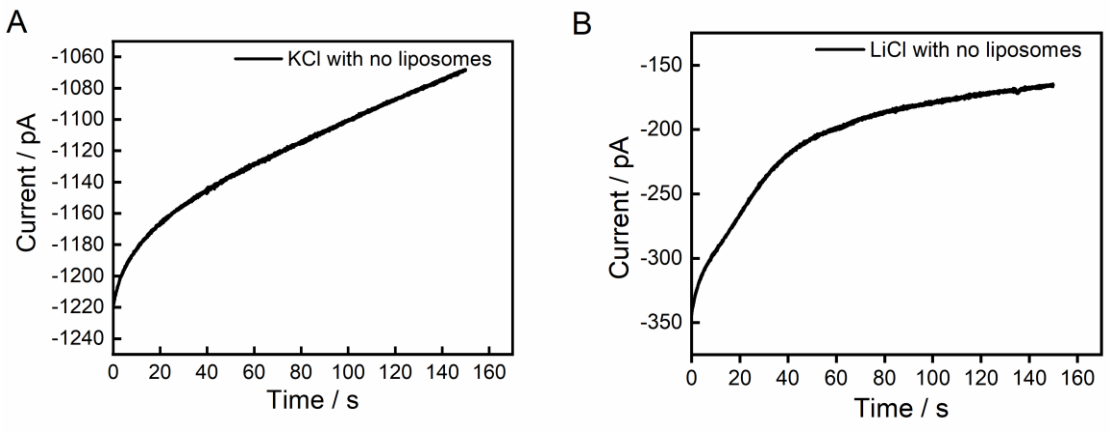


**Figure S5**. Representative *i*−*t* curves for micro-ITIES (i.d. = 6.5 and 7.7 μm for panels A and B, respectively) collisional experiments recorded at +0.6 V vs. Ag/AgCl in the absence of liposomes but with (A)10 mM KCl or with (B) 10 mM LiCl in the aqueous phase. The organic phase was 5 mM BATB + 0.5 mM DB18C6 in DCE.

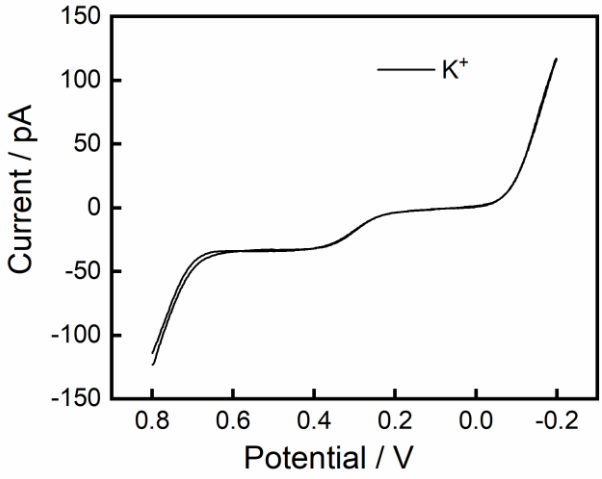


**Figure S6.** CV (scan rate: 20 mV $s^{-1}$) recorded at a micro-ITIES (i.d. = 600 nm), in which the aqueous phase was 10 mM KCl without ion-contained liposomes, and the organic phase was 5 mM BATB + 0.5 mM DB18C6 in DCE.

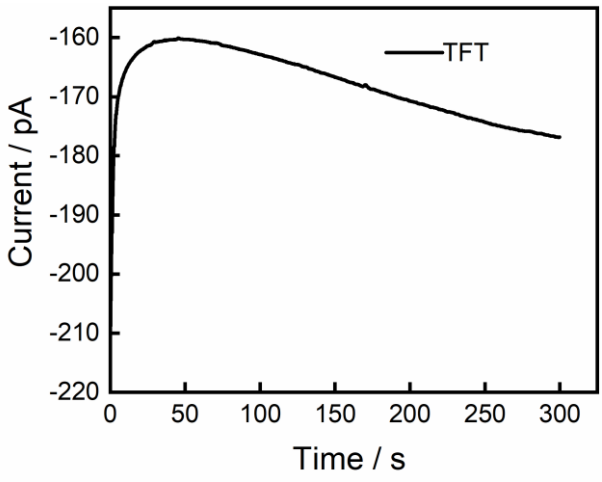


**Figure S7.** Representative *i*−*t* curve for a micro-ITIES (i.d. = 6.5 μm) collisional experiment recorded at +0.6 V vs. Ag/AgCl, in which the aqueous phase was $K^+$-loaded liposomes suspended in 10 mM LiCl, and the organic phase was 5 mM BATB + 0.5 mM DB18C6 in TFT.

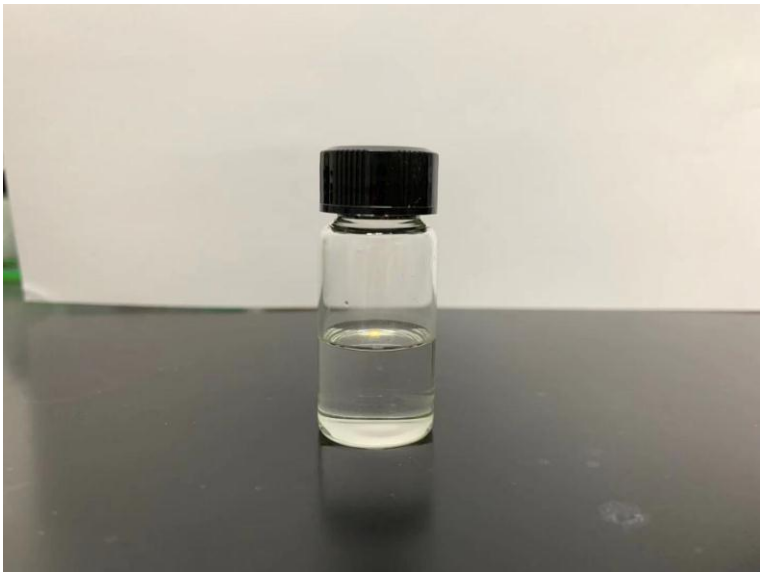

**Figure S8.** Photo of the 5 mL DCE dissolving with 7 mg of DOPC.

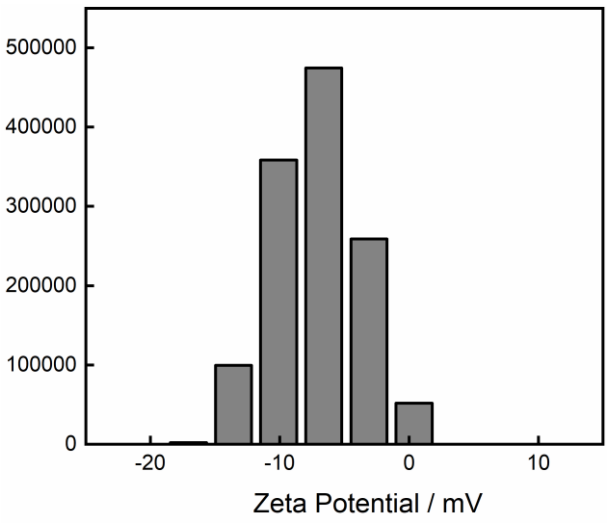


**Figure S9.** Histograms of the zeta potential of potassium-loaded liposomes suspended in 10 mM LiCl as determined by DLS.

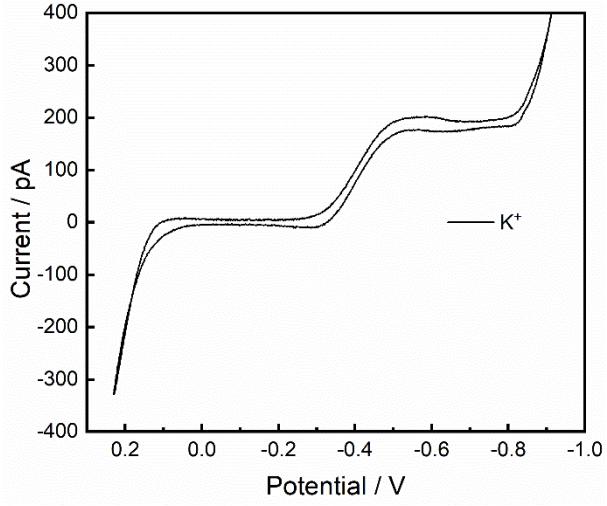


**Figure S10.** CV (scan rate: 20 mV $s^{-1}$) recorded at a micro-ITIES (i.d. = 1.6 μm), in which the aqueous phase was 10 mM LiCl and 0.5 mM KCl without ion-contained liposomes outside the pipette, and the organic phase was 5 mM BATB + 10 mM DB18C6 in DCE inside the pipette.

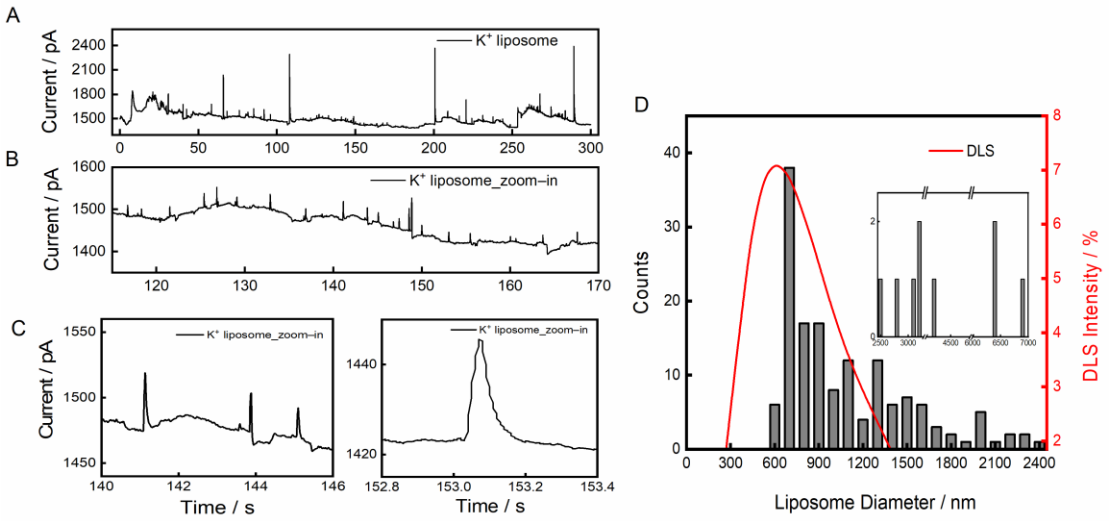


**Figure S11.** (A) Representative *i*−*t* curve recorded at –0.6 V vs. Ag/AgCl with Cell S-I for collisions of potassium-loaded liposomes onto a micro-ITIES supported at the orifice of a 6.3 μm-i.d. micropipette. The data was sampled every 5 ms. (B-C) Zoom-in ranges with different resolutions of 115–170 s, 140–146 s, and 152.8–153.4 s of the *i*−*t* curve shown in panel A. (D) Comparison of the liposome size distribution obtained by electrochemical collision detection (gray histogram) and that measured by DLS (red trace).

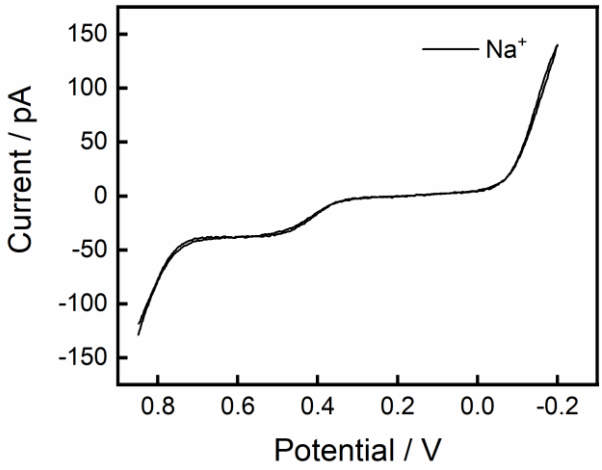


**Figure S12.** CV (scan rate: 20 mV $s^{-1}$) recorded at a micro-ITIES (i.d. = 600 nm), in which the aqueous phase was 10 mM NaCl without ion-contained liposomes, and the organic phase was 5 mM BATB + 0.5 mM DB18C6 in DCE.

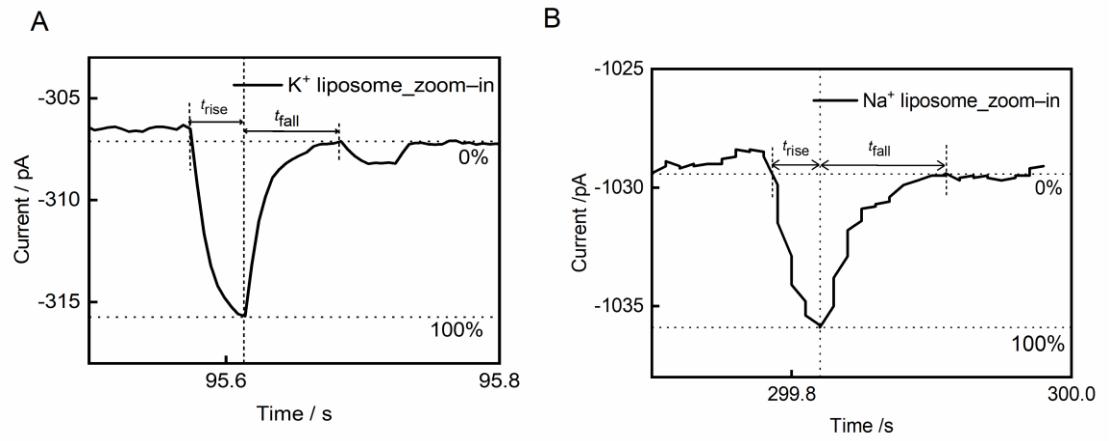


**Figure S13.** Typical current spike associated with a liposome loaded with either (A) potassium ion or (B) sodium ion. The micro-ITIES has i.d. = 6.4 and 10 μm for panels A and B, respectively; the other parameters were detailed in Figures 2 and 3 in the main text.

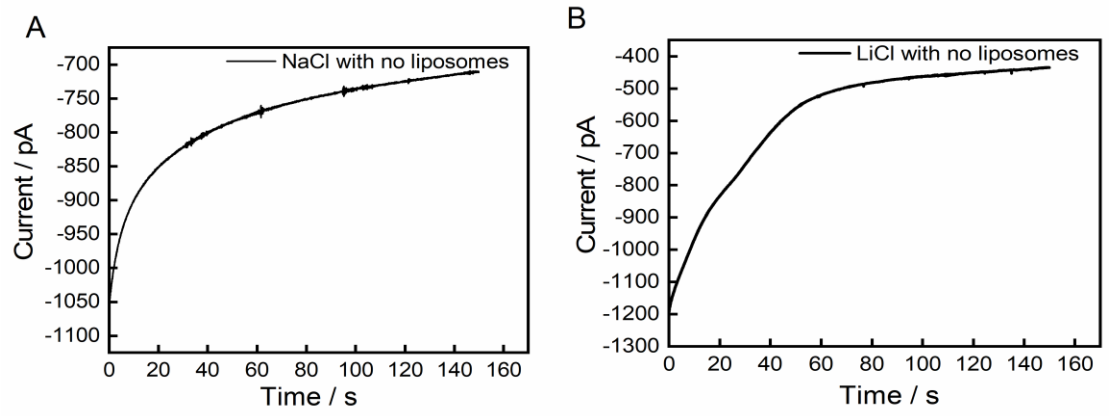


**Figure S14.** Representative *i*−*t* curves for micro-ITIES (i.d. = 9.0 and 6.7 μm for panels A and B, respectively) collisional experiments recorded at +0.75 V vs. Ag/AgCl, in which the aqueous phase was either (A) 10 mM NaCl or (B) 10 mM LiCl in the absence of liposomes, and the organic phase was 5 mM BATB + 0.5 mM DB18C6 in DCE.

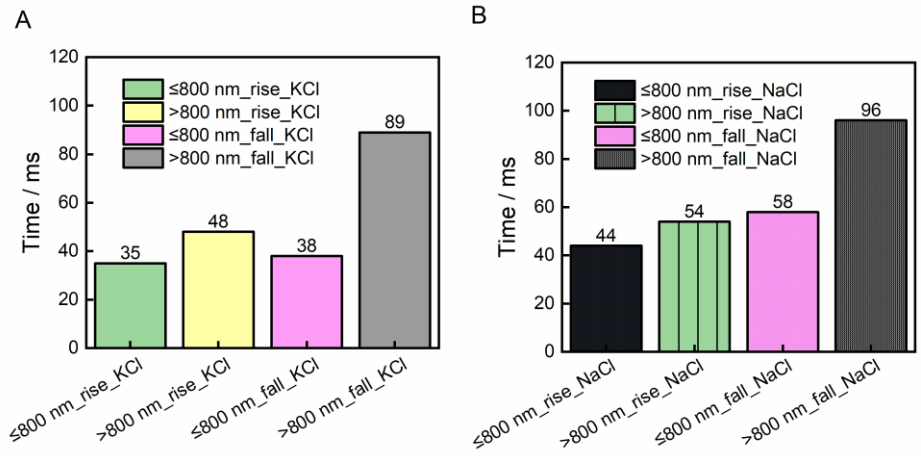


**Figure S15.** Histograms of $t_{rise}$ and $t_{fall}$ of collisions obtained from different-sized (A) potassium ion-loaded liposomes and (B) sodium ion-loaded liposomes. The other experimental conditions were detailed in the captions of Figures 2 and 3 in the main text.

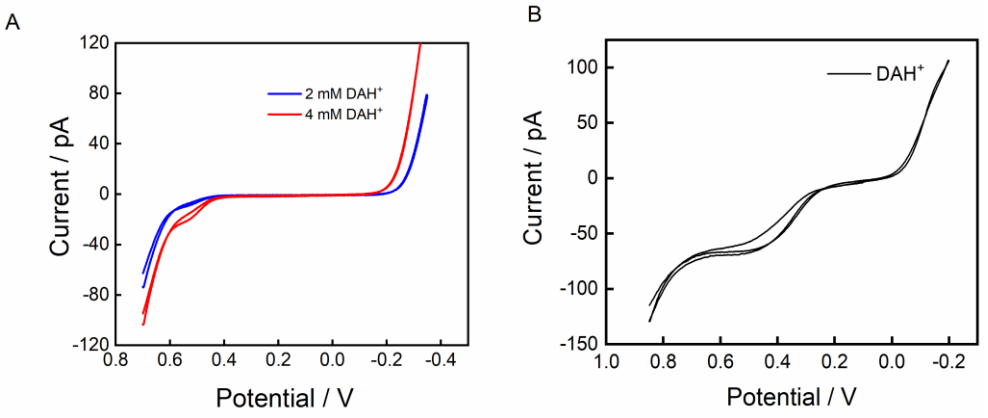


**Figure S16.** (A) CVs (scan rate: 20 mV $s^{-1}$) recorded at a micro-ITIES (i.d. = 600 nm), in which the aqueous phase was 10 mM LiCl with either 2 (blue trace), or 4 (red trace) mM DAHCl without ion-contained liposomes, and the organic phase was 5 mM BATB in DCE. (B) CV (scan rate: 20 mV $s^{-1}$) recorded at a micro-ITIES (i.d. = 600 nm), in which the aqueous phase was 10 mM DAHCl without ion-contained liposomes, and the organic phase was 5 mM BATB + 0.5 mM DB18C6 in DCE.

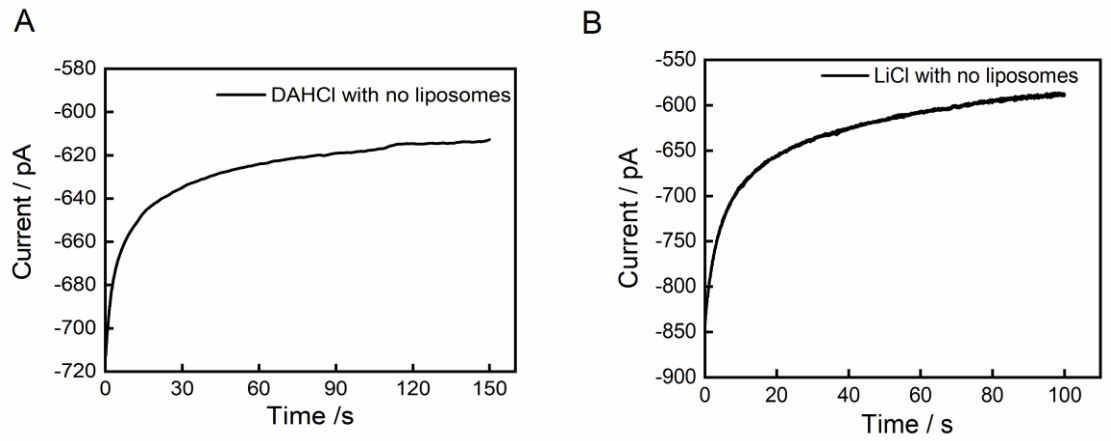


**Figure S17.** Representative *i*−*t* curves for micro-ITIES (i.d. = 5.4 and 7.5 μm for panels A and B, respectively) collisional experiments recorded at +0.85 V vs. Ag/AgCl, in which the aqueous phase was either (A) 10 mM DAHCl or (B) 10 mM LiCl in the absence of liposomes, and the organic phase was 5 mM BATB + 0.5 mM DB18C6 in DCE.

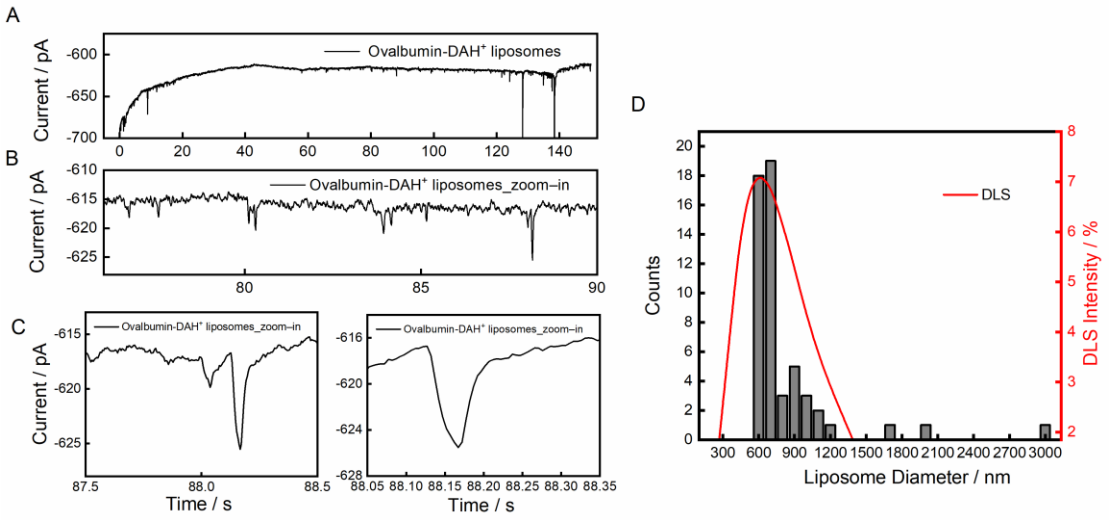


**Figure S18.** (A) Representative *i*−*t* curve recorded at +0.78 V vs. Ag/AgCl with Cell S-II for collisions of $DAH^+$-loaded ovalbumin-decorated liposomes at a micro-ITIES supported at the orifice of a 8.0 μm-i.d. micropipette. The data was sampled every 5 ms. (B-C) Zoom-in ranges with different resolutions of 76–90 s, 87.5–88.5 s, and 88.05–88.35 s of the *i*–*t* curve shown in panel A. (D) Comparison of the liposome size distribution obtained by electrochemical collision detection (gray histogram) and that measured by DLS (red trace).

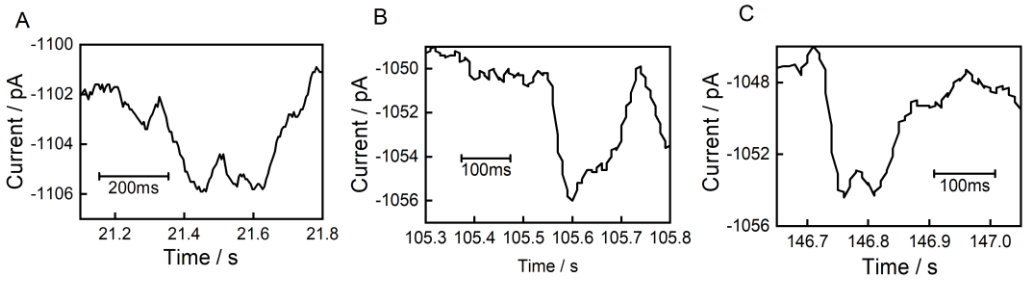


**Figure S19.** (A–C) More experimental results of observed multiplet events for sodium-ion loaded liposomes. The other experimental conditions were detailed in the caption of Figure 3 in the main text.

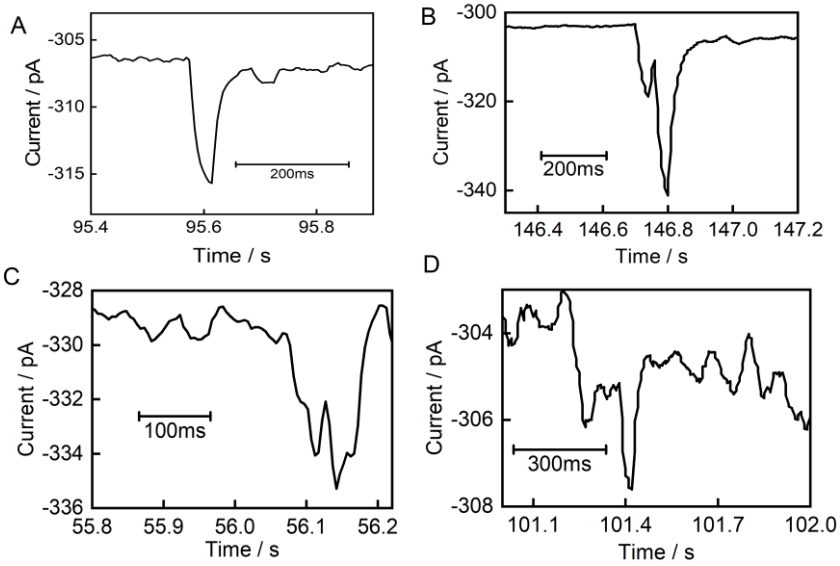


**Figure S20.** More experimental results of observed (A) singlet, (B) doublet, and (C-D) multiplet events for potassium-ion loaded liposomes. We stressed here that there was another category of multiplet events besides what we have introduced for the results of Figure 5 and related discussions in the main text. When the size of the pore opening increased over time during multiple flickering events, the current feature was expected as that shown in Figure S20 C,D, which was just the opposite of the pore changing process as shown in Figure 5D in the main text. In summary, the singlet event was the most common one with 95% occurrence frequency, the doublet event had 1% occurrence frequency, and the multiplet event occurred with 4% occurrence frequency. The other experimental conditions were detailed in the caption of Figure 2 in the main text.

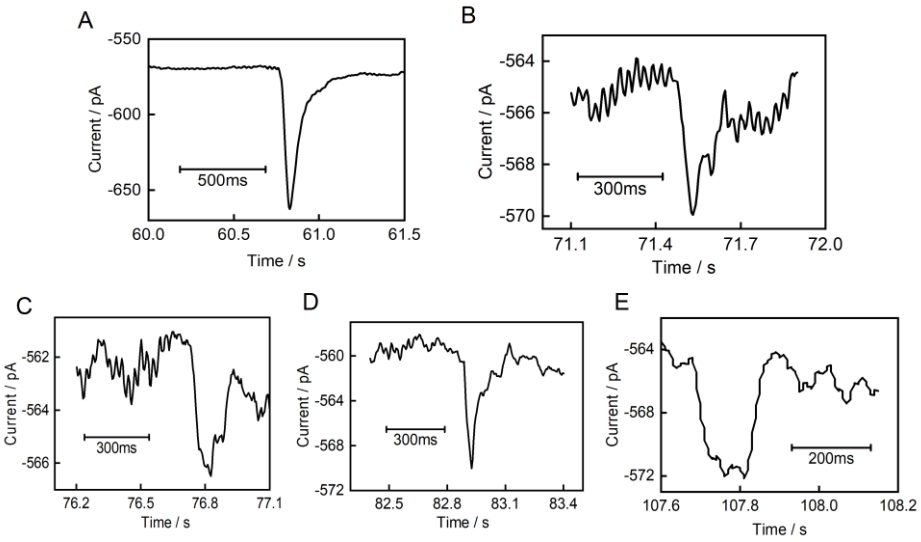


**Figure S21.** More experimental results of observed (A) singlet, (B) doublet, and (C–E) multiplet events for DAHCl-loaded liposomes. In summary, the singlet event was the most common one with 91% occurrence frequency, the doublet event had 2% occurrence frequency, and the multiplet event occurred with 7% occurrence frequency. The other experimental conditions were detailed in the caption of Figure 4 in the main text.